the plant journal

SEB Society for Experimental Biology

The Plant Journal (2017) doi: 10.1111/tpj.13589

The brassinosteroid receptor BRI1 can generate cGMP enabling cGMP-dependent downstream signaling

Janet I. Wheeler[1,2,†], Aloysius Wong[3,4], Claudius Marondedze[3,5], Arnoud J. Groen[5], Lusisizwe Kwezi[1,6], Lubna Freihat[1], Jignesh Vyas[1], Misjudeen A. Raji[7], Helen R. Irving[1,*] and Chris Gehring[3]

[1]*Monash Institute of Pharmaceutical Sciences, Monash University, Melbourne, VIC 3052, Australia,*

[2]*AgriBio, La Trobe University, Bundoora, VIC 3083, Australia,*

[3]*Division of Biological and Environmental Science and Engineering, King Abdullah University of Science and Technology, Thuwal, Saudi Arabia,*

[4]*College of Natural, Applied and Health Sciences, Wenzhou-Kean University, 88 Daxue Road, Ouhai, Wenzhou, Zhejiang Province, China 325060,*

[5]*Cambridge Centre for Proteomics, Department of Biochemistry, University of Cambridge, Cambridge, UK,*

[6]*Council for Scientific and Industrial Research, Biosciences, Brummeria, Pretoria 0001, South Africa, and*

[7]*Analytical Chemistry Core Laboratory, King Abdullah University of Science and Technology, Thuwal, Saudi Arabia*

Received 24 January 2017; revised 20 April 2017; accepted 21 April 2017.

*For correspondence (e-mail helen.irving@monash.edu).

[†]Present address: AgriBio, Centre for AgriBioscience, La Trobe University, Bundoora, VIC, 3083, Australia.

SUMMARY

The brassinosteroid receptor brassinosteroid insensitive 1 (BRI1) is a member of the leucine-rich repeat receptor-like kinase family. The intracellular kinase domain of BRI1 is an active kinase and also encapsulates a guanylate cyclase catalytic centre. Using liquid chromatography tandem mass spectrometry, we confirmed that the recombinant cytoplasmic domain of BRI1 generates pmol amounts of cGMP per μg protein with a preference for magnesium over manganese as a co-factor. Importantly, a functional BRI1 kinase is essential for optimal cGMP generation. Therefore, the guanylate cyclase activity of BRI1 is modulated by the kinase while cGMP, the product of the guanylate cyclase, in turn inhibits BRI1 kinase activity. Furthermore, we show using Arabidopsis root cell cultures that cGMP rapidly potentiates phosphorylation of the downstream substrate brassinosteroid signaling kinase 1 (BSK1). Taken together, our results suggest that cGMP acts as a modulator that enhances downstream signaling while dampening signal generation from the receptor.

Keywords: *Arabidopsis thaliana*, brassinosteroid receptor (BRI1), cGMP, kinase, guanylate cyclase, brassinosteroid signaling kinase 1 (BSK1).

INTRODUCTION

The plant hormone brassinosteroid controls plant growth and development, and in Arabidopsis is perceived by the leucine-rich repeat receptor kinase brassinosteroid insensitive 1 (BRI1). BRI1 is a single membrane spanning receptor kinase that when bound by the brassinosteroid, brassinolide, induces heterodimerization with BRI1-associated receptor kinase (BAK1)/somatic embryogenesis receptor-like kinase 3 (SERK3). This association brings the cytoplasmic C-termini of both molecules into close proximity (Clouse, 2011; Hothorn *et al.*, 2011; Sun *et al.*, 2013) allowing for auto and trans-phosphorylation of both BRI1 and BAK1 and the subsequent phosphorylation of the downstream targets BRI1 substrate kinases (BSKs) (Tang *et al.*, 2008; Sreeramulu *et al.*, 2013) and constitutive differential growth 1 (CDG1) (Kim *et al.*, 2011) that are involved in activating several transcription factors to regulate brassinosteroid dependent gene expression. Although many elements of the brassinosteroid pathway have been extensively studied it remains unclear how the BRI1 kinase domain switches from its inactive basal to its phosphorylation capable activated state, which allows phosphorylation of partners and downstream targets and how it is in turn down-regulated back to the basal state.

Protein regulation is essential in all living organisms to ensure correct spatial and temporal protein expression but also for regulation in response to environmental cues

particularly in plants as they are sessile. Recent improvements in imaging resolution have identified restricted localization of signaling molecules within cellular cytoplasmic areas in microdomains or microenvironments such as the *Solanum tuberosum* sucrose transporter SUT1 (Krügel *et al.*, 2008) or *Medicago truncatula* lysine motif receptor like kinase 3 (LYK3; (Haney *et al.*, 2011). Considering that cellular interiors are crowded with densely packed proteins (Fulton, 1982; Spitzer and Poolman, 2013), it is only natural that signaling molecules are restricted to microenvironments that contain a complex of scaffold and interacting proteins.

Cyclic GMP (cGMP) is a key signaling intermediate in eukaryotes, including higher plants, in which a diverse group of responses is dependent on cGMP including changes in ion movement, phosphoproteome and transcriptome (Maathuis, 2006; Isner *et al.*, 2012; Facette *et al.*, 2013; Marondedze *et al.*, 2016b). Using a rationally designed search motif, we identified and experimentally confirmed a number of molecules with guanylate cyclase (GC) activity. Some of these molecules are receptor-like kinases that have the GC catalytic centre embedded within subdomain IX of the kinase domain and *in vitro* studies have shown that BRI1 (Kwezi *et al.*, 2007), phytosulfokine receptor 1 (PSKR1) (Kwezi *et al.*, 2011; Muleya *et al.*, 2014) and PePR1 (Qi *et al.*, 2010) all have GC activity. In addition, we have since shown that PSKR1 kinase and GC activity is reciprocally modulated by calcium (Muleya *et al.*, 2014).

Here we report that the ability of the kinase domain of BRI1 to generate cGMP depends on its kinase catalytic ability. Furthermore, we show that cGMP stimulates phosphorylation of BSK1. Therefore, we propose that cGMP acts as a modulator to stimulate activation of downstream phosphorylation of members of the BRI1 signaling pathway.

RESULTS AND DISCUSSION

BRI1 generates cGMP

Previously, we have shown that a small 114 amino acid fragment of the BRI1 cytoplasmic domain recombinant protein ($BRI1^{1012–1134}$) has a predicted GC catalytic centre that enabled GC activity (Figure 1a). We assessed cGMP generated by the $BRI1^{1012–1134}$ using the cGMP enzyme immunoassay assay (EIA) Biotrak system (GE Healthcare, USA) and confirmed this with mass spectrometry (Kwezi *et al.*, 2007). We later demonstrated that brassinolide induces an increase in cGMP in wild-type freshly isolated protoplasts using the EIA system (Irving *et al.*, 2012). However, a recent study using a longer portion of the intracellular domain of the recombinant protein ($BRI1^{865–1160}$) containing the kinase domain reported that GC activity could not be detected with UV absorbance (Bojar *et al.*, 2014). As the original construct used was a fragment, it is possible that it could more readily fold as a GC than the longer construct that assumes typical kinase folds crystallised by (Bojar *et al.*, 2014). In addition, mass spectrometry determination of cGMP is far more sensitive and accurate than either the cGMP enzyme immunoassay assay or the UV detection of HPLC separated fractions (used by Bojar *et al.*, 2014). In order to address this discrepancy, we undertook liquid chromatography tandem mass spectrometry (LC-MS/MS) to evaluate cGMP production by the cytoplasmic domain recombinant protein, $BRI1^{815–1196}$ and specifically identified the presence of the unique product ion at m/z 152.06 $[M+H]^+$ that is obtained via High Collision Dissociation (HCD) of the protonated cGMP precursor ion (m/z 346.06). This product ion was then used for quantitation. $BRI1^{815–1196}$, which represents the longest fragment characterized to-date, generates 7.10 ± 0.29 pmol of cGMP per μg protein. In addition, we observed a strong preference for magnesium as a co-factor rather than manganese, which results in 0.63 ± 0.03 pmol of cGMP per μg protein (Figure 1b, c). The superimposed extracted mass chromatograms of m/z 346.06 $[M+H]^+$ ion of cGMP all have the corresponding product ion at m/z 152.06 $[M+H]^+$ and this confirmed the presence of cGMP in the reaction mixtures of the respective recombinant BRI proteins (Figure 1b, c). Similar amounts of cGMP are generated by the recombinant cytoplasmic domain and the full-length PSKR1 (Kwezi *et al.*, 2011; Muleya *et al.*, 2014, 2016). It is noteworthy that a recently characterized adenylate cyclase from Arabidopsis (AtKUP7) also has activity resembling that of plant GCs (Al-Younis *et al.*, 2015). We therefore conclude that these pmol amount of cyclic nucleotide products per μg recombinant protein determined by the sensitive high resolution mass spectrometry method, is accurate and presumably reflective of physiological conditions. Considering that plant cells have relatively small cytoplasmic interiors, it is only natural that signaling molecules are restricted to microenvironments that contain a complex of scaffold and interacting proteins. Moreover, an Arabidopsis plant natriuretic peptide receptor (AtPNP-A) generates similar amounts of cGMP that in turn affect plant salt and water balance and responses to biotrophic plant pathogens (Turek and Gehring, 2016) indicating that these low amounts of cGMP are physiologically relevant. It was previously reported (Bojar *et al.*, 2014) that no cGMP is produced by the recombinant protein ($BRI1^{865–1160}$) when using UV absorbance as a method of detection of cGMP. However, using the far more sensitive tandem mass spectrometry method and microgram amounts of a slightly longer recombinant cytoplasmic domain $BRI1^{815–1196}$ protein we unambiguously demonstrate that cGMP is produced. This difference could be due to the fact that our constructs include the N and C terminal domains necessary for *in vitro* dimerization as determined by

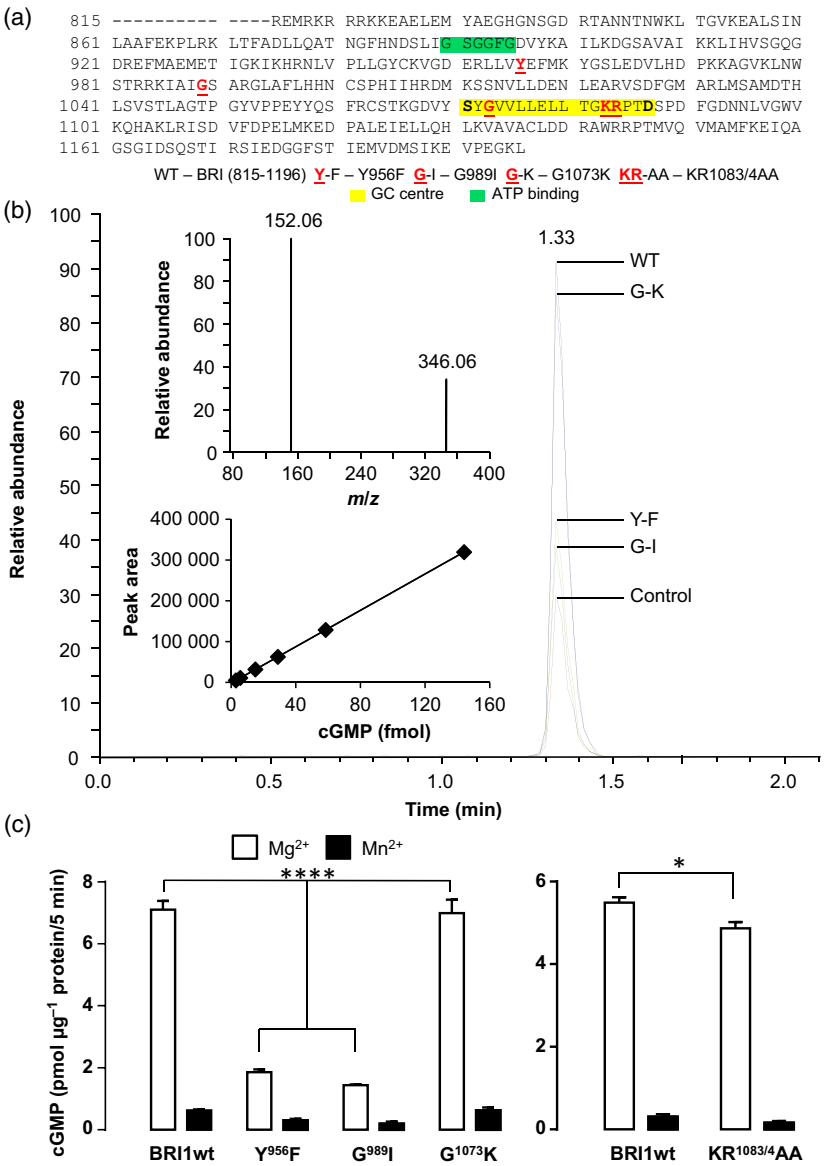

Figure 1. Detection of cGMP generated by wild-type and mutant recombinant BRI by liquid chromatography tandem mass spectrometry (LC-MS/MS).

(a) Amino acid sequence of recombinant BRI (Val^{815}–Leu^{1196}) showing the domain organization of the ATP binding site (green) and GC centre (yellow). The functional residues in the GC catalytic centre are indicated in bold while the red underlined residues are mutated for functional studies.

(b) Five superimposed ion chromatograms of cGMP (m/z 346 $[M+H]^+$) generated by 5 µg recombinant $BRI1^{815–1196}$ (black), $BRI1^{815–1196}$Y956F (yellow), $BRI1^{815–1196}$G989I (green), $BRI1^{815–1196}$ G1073K (blue) protein and control (no protein, red) after 5 min in the presence of 5 mM Mg^{2+}. The lower inset shows the cGMP calibration curve performed with 2.88–144.10 fmoles of pure cGMP on the column. The upper inset shows the parent cGMP ion at m/z 346 $[M+H]^+$ and the corresponding product ion after HCD (higher energy collision-induced dissociation) fragmentation at m/z 152 $[M+H]^{+1}$ which is used for quantitation.

(c) Amount of cGMP produced per recombinant protein as determined by mass spectrometry. Reaction mixture containing 5 µg of recombinant protein ($BRI1^{815–1196}$, $BRI1^{815–1196}$Y956F, $BRI1^{815–1196}$G989I or $BRI1^{815–1196}$ G1073K) in 50 mM Tris (pH 7.5), 2 mM isobutyl methylxanthine (IBMX), 1 mM GTP with either 5 mM Mg^{2+} or 5 mM Mn^{2+} was incubated for 5 min prior to cGMP detection by LC-MS/MS and the results are shown in the left panel. Independent analyses of cGMP generation were undertaken as described above with $BRI1^{815–1196}$ and $BRI1^{815–1196}$KR1083/4AA and the results are shown in the right panel. cGMP amounts generated by at least two biologically independent clones for each BRI protein were considered. LC-MS/MS was performed in triplicate and the cGMP values were averaged with the error bars representing standard error of the mean. Data were analysed by two-way ANOVA followed by Sidak's multiple comparisons post-*hoc* test.

crystallization (Bojar *et al.*, 2014). Consistent with this consideration, we previously discussed (Freihat *et al.*, 2014) that dimerization is likely to be a prerequisite for guanylate cyclase activity. Soluble monomeric guanylate cyclase subunits are believed to form head-to-tail asymmetric dimers containing metal-binding and transition state-stabilising residues along the intermolecular interface forming the catalytic cleft for GTP binding (Rauch *et al.*, 2008; Winger *et al.*, 2008; Allerston *et al.*, 2013). Molecular docking of GTP to the GC catalytic centre of the BRI1 GC (Leu^{1021}–Arg^{1134}) model reveals the substrate pose and interactions with key residues serine, arginine and aspartic acid of the GC centre (Figure 2a), which closely resembles that of the PSKR1 GC centre (Wong and Gehring, 2013; Wong *et al.*, 2015).

Kinase activity is necessary for cGMP production

To investigate if the kinase activity of the protein influences GC activity, we also generated two kinase dead BRI1 mutants; $BRI1^{815–1196}$Y956F and $BRI1^{815–1196}$G989I. $BRI1^{815–1196}$Y956F simulates the Y956F mutant described by (Oh *et al.*, 2009) who showed that this tyrosine residue in subdomain V of the kinase domain and is essential for kinase activity. We show that this Y956F mutation causes a three-fold reduction in guanylate cyclase activity to 1.85 ± 0.10 pmol of cGMP per µg protein with a similar preference for magnesium over manganese, 0.30 ± 0.05 pmol of cGMP per µg protein, as co-factor (Figure 1c). As phenylalanine and tyrosine are about the same size, the reduction in GC activity is therefore attributed to

the additional reactive hydroxyl group of tyrosine, which allows for interaction with non-protein atoms and importantly for phosphorylation events (Figure 2b). We note that the Y956 residue is situated deep into the cavity of the kinase catalytic centre (Figure 2b) and importantly, this residue has been previously identified as an auto-phosphorylation site (Oh *et al.*, 2009). BRI1$^{815–1196}$G989I simulates the *bri1-301* mutant isolated by (Xu *et al.*, 2008). The *bri1-301* mutation has a two base alteration from GG to AT which causes glycine 989 to become isoleucine in the kinase domain (within the IVa subdomain) and the mutated plants show moderate morphological phenotypes and a reduced response to brassinosteroids. *In vitro* assays were used (Xu *et al.*, 2008) to show that *bri1-301* has no detectable autophosphorylation activity or phosphorylation activity towards BAK1 or transthyretin-like (TTL). In our hands BRI1$^{815–1196}$G989I also has reduced GC activity, generating only 1.44 $\pm$ 0.02 pmol/μg protein and the same preference for magnesium over manganese as the co-factor. When isoleucine takes the place of glycine at position 989, it orientates itself towards an opposing β-sheet causing increased strain with reduced structural flexibility and also increased the overall hydrophobicity in a compact region at the rear of the protein (Figure 2b). Such changes may account for the reduced GC activity of the BRI1$^{815–1196}$G989I as structural flexibility in particular is an important feature for multi-functional proteins to allow the switch from one activation state to another as occurs with PSKR1 (Muleya *et al.*, 2014). Notably wild-type BRI1 has strong autophosphorylation activity resulting in heavily phosphorylated recombinant protein whereas both BRI1$^{815–1196}$Y956F and BRI1$^{815–1196}$G989I being 'kinase dead' mutants lack phosphorylated residues (Xu *et al.*, 2008; Oh *et al.*, 2009). Whether the reduction in GC activity observed in the BRI1 mutants is due to lack of kinase activity or lack of phosphorylated residues remains to be investigated. A recent study with recombinant cytoplasmic domain of PSKR1 suggests that the phosphorylation status may be more important as mutations to the kinase active site that inhibited kinase activity did not modulate GC activity (Muleya *et al.*, 2016).

The GC catalytic centres contain conserved residues involved in selecting specific nucleotides and stabilising the transition state to form the cyclic nucleotide. In BRI1, the GC centre resides in residues 1071–1084 where the glycine at 1073 is predicted to confer substrate selectivity for GTP (Wong *et al.*, 2015). Previously, we showed that mutations at position 3 of the GC catalytic centre in the recombinant cytoplasmic domain of PSKR1 resulted in marked changes in cGMP production with a G:K mutation suppressing and G:E mutation enhancing cGMP production (Kwezi *et al.*, 2011; Muleya *et al.*, 2014). Interestingly, complementation of *pskr1/pskr2* null mutant plants with full-length PSKR1^{G923K} does not rescue the short root phenotype unlike complementation with wild-type receptor (Ladwig *et al.*, 2015). We created the BRI1$^{815–1196}$G1073K and observed that the recombinant BRI1$^{815–1196}$G1073K shows no change in GC activity and the same preference for magnesium as a co-factor over manganese 7.00 $\pm$ 0.43 pmol/μg protein (Mg) and 0.63 $\pm$ 0.09 pmol/μg protein (Mn) (Figure 1c). We observed that in the BRI model incorporating the G1073K mutation, the lysine residue was orientated so that the positively charged side chain is pointing towards the negatively charged phosphates of GTP suggesting stabilising interactions in the presence of the substrate. In addition, there appears to be sufficient space to accommodate the increased bulkiness of lysine orientated in this manner (Figure 2b). These are possible reasons for why the GC activity of the BRI1$^{815–1196}$G1073K mutant does not alter from the wild-type. Here, we also show in the BRI model that G1073E mutation results in the negative side chain of glutamic acid pointing towards the guanosine of GTP and as there is also sufficient space to accommodate this orientation (Figure 2b), this change should not negatively affect the GC activity of BRI1. A second mutant in the GC centre BRI1$^{815–1196}$KR1083/4AA was created and the recombinant BRI1$^{815–1196}$KR1083/4AA protein has slight but statistically significant reduction of cGMP production of 4.86 $\pm$ 0.155 pmol/μg protein in comparison to the wild-type BRI1$^{815–1196}$ recombinant protein at 5.49 $\pm$ 0.132 pmol/μg protein (Figure 1c). A BRI model incorporating the KR1083/4AA mutations was able to form a helical structural fold (Figure S1) that characterizes all Arabidopsis GC centres reported to-date (Wong *et al.*, 2015) and thus may account for the presence of GC activity albeit at a lowered rate. This observation implied that these positively charged amino acid residues at the GC centre which have been previously identified as key residues for interactions with the phosphate group of the GTP substrate (Wong and Gehring, 2013; Marondedze *et al.*, 2016a), are required for optimal catalysis.

Modulation of BRI1 kinase activity

As the kinase dead mutants no longer produced cGMP, we also considered the role of the GC centre in modulating kinase activity. To ensure that we were measuring specific BRI1 kinase activity, we used the BR13 peptide as a substrate (Oh *et al.*, 2000). Recombinant BRI1$^{815–1196}$ wild-type protein effectively phosphorylated the BR13 peptide substrate and as expected the kinase dead BRI1$^{815–1196}$Y956F mutant did not (Figure 3a). The recombinant BRI1$^{815–1196}$KR1083/4AA, which has reduced GC activity, also consistently showed a reduced ability to phosphorylate the BR13 substrate although it was not significantly different from the wild-type control or the BRI1$^{815–1196}$Y956F mutant (Figure 3a). This is similar to PSKR1 in which mutations in the GC catalytic centre in the recombinant cytoplasmic

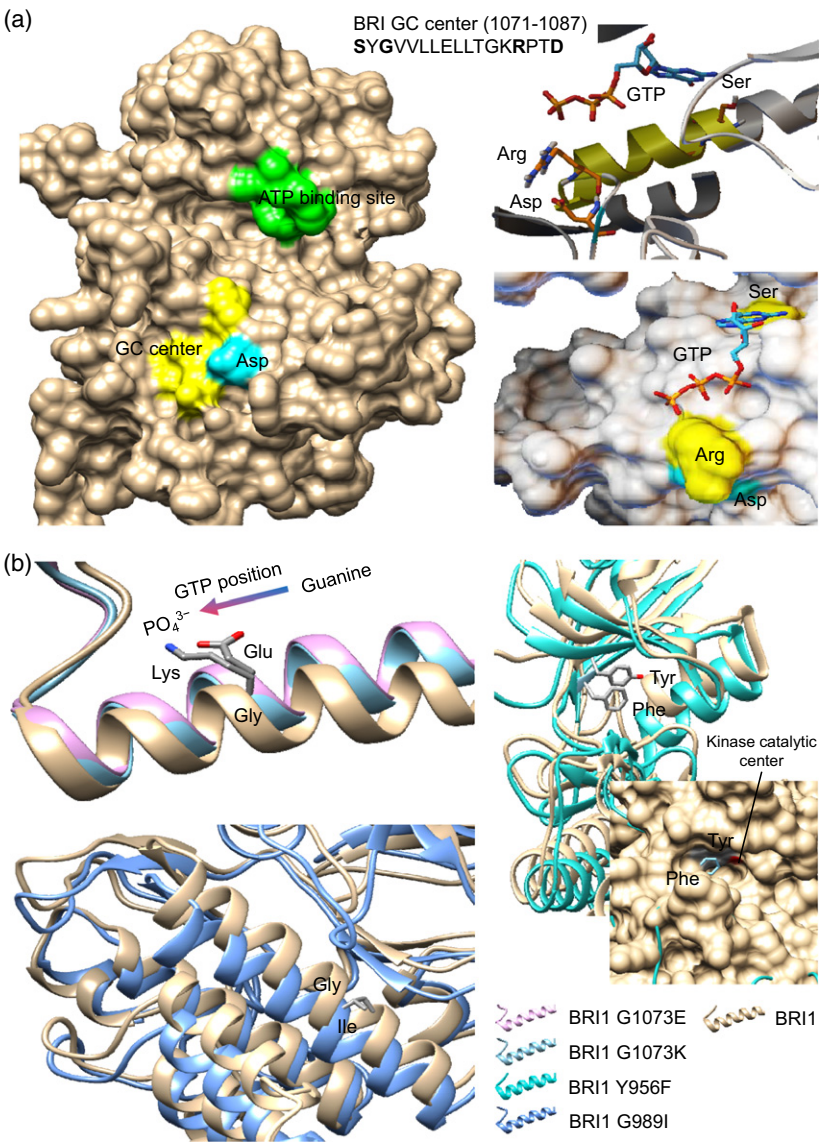

Figure 2. Probing the structure of BRI1 (Arg^{815}–Leu^{1196}) by computational methods.
(a) The homology model of the kinase domain of BRI1 (Arg^{815}–Leu^{1196}) shows the domain organizations of the ATP binding site (green) and the GC catalytic centre (yellow). Molecular docking of GTP to the GC centre (right panel) of the BRI1 GC (Leu^{1021}–Arg^{1134}) model reveals the substrate pose and interactions with key residues (bold) of the GC centre. Yellow and cyan coloured ribbon and surface represents the GC catalytic centre and metal-binding residue.
(b) Ribbon models of BRI1 (Arg^{815}–Leu^{1196}) incorporating the mutations G1073K and G1073E (upper left) were superimposed and they show the orientations of the introduced residues at the GC centre. The models incorporating mutations at G989I (ribbon, lower left) and Y956F (ribbon and surface, upper right) were compared to the non-mutated $BR1^{815–1196}$ model. Homology models of BR1 kinase domain (Arg^{815}–Leu^{1196}) and BRI1 GC centre (Leu^{1021}–Arg^{1134}) were based on the crystal structure of the BRI1 kinase domain (PDB entry: 4OA2) which has a sequence similarity of 98% covering 87% of the queried amino acid sequence. Models were built and assessed using Modeller (ver. 9.14) (Sali and Blundell, 1993) and GTP docking simulation was performed using AutoDock Vina (ver. 1.1.2) (Trott and Olson, 2010). All structures and images were analysed and prepared with UCSF Chimera (Pettersen *et al.*, 2004) and PyMOL (ver. 1.7.4) (The PyMOL Molecular Graphics System, Schrödinger, LLC).

domain that reduce cGMP production do not significantly alter kinase activity although it is reduced (Muleya *et al.*, 2014). Although both PSKR1 and BRI1 are in the same LRR-Xb family (Shiu *et al.*, 2004), it is conceivable that the precise interactions between the kinase and GC catalytic centre diverge in the different proteins and that this is dependent upon phosphorylation status. Indeed phosphorylation status of PSKR1 and/or its kinase activity is important in modulating the ability of the recombinant protein to generate cGMP. Mutations in the juxtamembrane position suppressed GC activity despite alternative effects on kinase activity whereas mutations in the active site that abolished kinase activity had no effect on GC activity (Muleya *et al.*, 2016). We transiently expressed GFP-tagged full-length wild-type BRI1, BRI1Y956F and BRI1KR1083/4AA in tobacco. Full-length GFP-tagged wild-type and mutant proteins were isolated by immunoprecipitation and detected by immunoblot analysis. Immunoprecipitated proteins were incubated with myelin basic protein in the presence of ATP and then separated by SDS-PAGE. Both wild-type and the BRI1KR1083/4AA mutant consistently enhanced phosphorylation of myelin basic protein, whereas phosphorylation was lower with the BRI1Y956F mutant as expected (Figure 3b). Although the results possibly indicate that BRI1KR1083/4AA has greater kinase activity *in planta* than *in vitro*, it should be treated cautiously as different substrates were used in the two assays.

So what is the role of cGMP and how does cGMP fit in the broader signaling regulatory mechanisms of BRI1? One possibility is that cGMP is acting as a 'tonic' on the protein and its immediate environs. To test this notion, we determined the effect of cGMP on the kinase activity of wild-

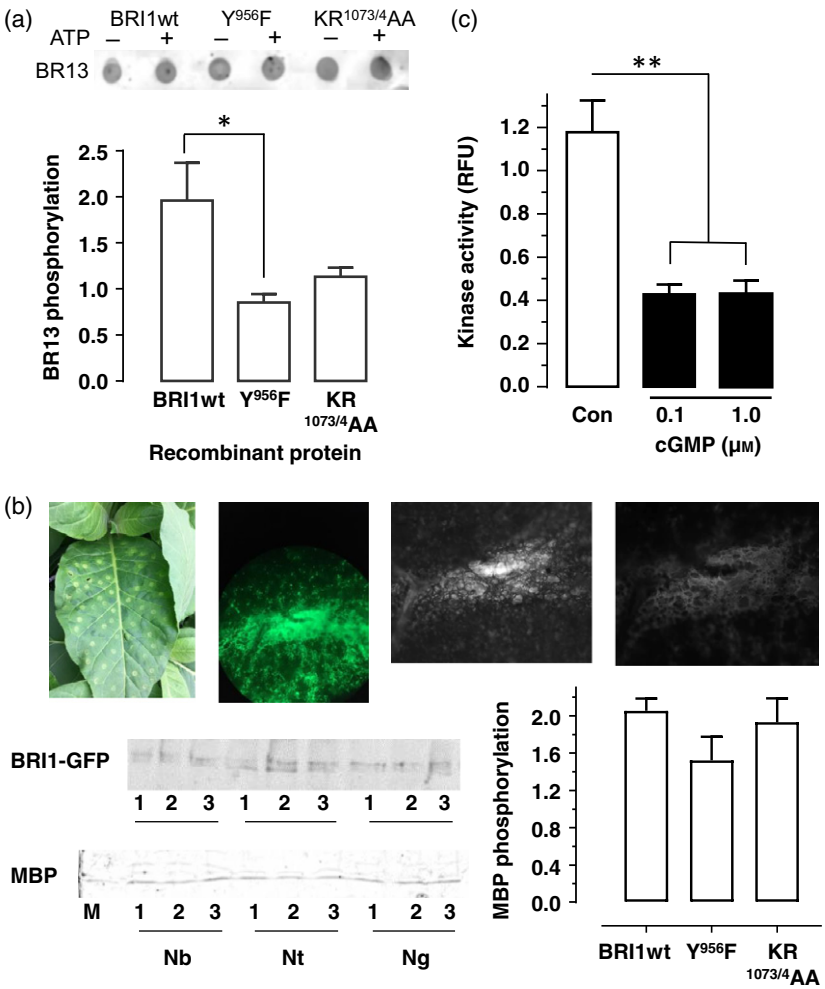

Figure 3. BRI1 kinase activity is inhibited by mutations and cGMP.
(a) Mutations in BRI1$^{815–1196}$ affect its ability to phosphorylate the BR13 peptide substrate. The upper panel shows a typical example of BR13 peptide stained by the Pro-Q phosphoblot stain following incubation in the presence or absence of 5 mM ATP and the specified recombinant protein. The lower panel shows the relative change in signal in the presence of ATP correlating to phosphorylation of BR13 peptide. Data were analysed by one-way ANOVA followed by Sidak's post-*hoc* test (*$P < 0.05$). The error bars represent standard error (SE) from eight to 10 separate assays using at least two independent protein preparations.
(b) Transiently expressed GFP-tagged full-length BRI1KR1083/4AA phosphorylates myelin basic protein (MBP). Representative *Nicotiana tabacum* (*Nt*) leaf infiltrated with transiently expressed GFP-tagged full-length BRI1 (top left), colour image of GFP expression of the same leaf (top middle left), bright field (top middle right) and GFP filter (top right) of the same leaf. Immunoblot of extracted transiently expressed GFP-tagged full-length BRI1(1), BRI1Y956F (2) or BRI1KR1083/4AA (3) immunoprecipitated from *Nicotiana benthamiana* (*Nb*), *Nicotiana tabacum* (*Nt*) or *Nicotiana glutinosa* (*Ng*) (middle left). Independent Pro-Q Diamond phosphoprotein stained blot of myelin basic protein (MBP) incubated with transiently expressed GFP-tagged full-length BRI1(1), BRI1Y956F (2) or BRI1KR1083/4AA (3) immunoprecipitated from *Nicotiana benthamiana* (*Nb*), *Nicotiana tabacum* (*Nt*) or *Nicotiana glutinosa* (*Ng*) and ATP (bottom left). BRI1 and BRI1KR1083/4AA show increased phosphorylation of MBP compared to MBP alone whereas BRI1Y956F was lower (bottom right). The graph is the average of MBP phosphorylation corrected for average variation in loading derived from GFP immunoblots and error bars represent standard error (SE) from three to five independent leaf infiltrations from three different *Nicotiana* spp.
(c) cGMP suppresses the kinase activity of BRI1$^{815–1196}$. Recombinant BRI1$^{815–1196}$ kinase activity was determined using the Ser/Thr peptide 1 as a substrate and measuring activity with the Omnia kinase assay. Data were analysed by one-way ANOVA followed by Holm–Sidak post-hoc test (**$P < 0.01$). All experiments were performed in triplicate, and error bars represent SE of a representative experiment from two independent assays.

type BRI1$^{815–1196}$. We used the Ser/Thr peptide 1 as a substrate and measuring activity with the Omnia kinase assay and show that wild-type BRI1$^{815–1196}$ has a K_m of ~7.5 μM (Figure S2) which is similar to recombinant PSKR1 (Kwezi *et al.*, 2011) using this system albeit lower than that reported for BR13 (Oh *et al.*, 2000). Interestingly, we observed that the kinase activity of BRI1$^{815–1196}$ is suppressed by cGMP (Figure 3c). A similar effect is seen on the kinase activity of PSKR1 (Kwezi *et al.*, 2011) indicating that cGMP may act to switch down kinase activity in receptor kinase molecules as a type of homeostatic control mechanism. At this stage we can only speculate on the mechanics underpinning the inhibitory effect. One possibility is that a portion of the generated cGMP remains bound

at the GC catalytic centre while BRI1 is in a still active kinase configuration. As more cGMP gets released into the immediate environs, a feedback response occurs where cGMP inhibits the kinase.

cGMP stimulates downstream phosphorylation signals in plant cells

Intracellular changes in cGMP have been associated with activation of ion channels, changes in the transcriptome and phosphorylation of proteins (Maathuis, 2006; Isner *et al.*, 2012; Facette *et al.*, 2013; Marondedze *et al.*, 2016b). To investigate if cGMP modified any downstream phospho-targets of BRI1, we treated Arabidopsis root cell cultures with 100 nM cGMP for 5 min before extracting all proteins, enriching for phosphopeptides and identifying differentially phosphorylated proteins (Marondedze *et al.*, 2016b). One of the cGMP-induced phosphoproteins identified was BSK1 phosphorylated on serine 230 (SYpSTNLAYTPPEYLR; Figure 4) and threonine 353 (KQEEAPSpTPQRPLSPLGEACSR; Figure S3). Previously, BSK1 was identified as a substrate of BRI1 by quantitative proteomics with the major phosphorylated residue being serine 230 (Tang *et al.*, 2008). Using bifluorescence complementation and co-immunoprecipitation studies Tang *et al.* (2008) showed that BRI1 and BSK1 interacted *in vivo*. Following activation of BRI1 via brassinosteroid and dimerization with BAK1, BRI1 phosphorylates BSK1 which then disassociates from the BRI1-BAK1 complex. Previously a phosphopeptide containing phosphorylated threonine 353 was identified in a large-scale screen of Arabidopsis shoots (Reiland *et al.*, 2009). Although several other proteins were phosphorylated, they could not be statistically correlated due to variability between biological replicates.

Our findings therefore implicate cGMP as an important and previously unidentified component of this signaling cascade. As the production of cGMP is relatively low, its effects are most likely to be evident in the immediate intracellular environment of BRI1 where it is being produced. BSKs are pseudokinases that are thought to act as adaptor or scaffold type proteins as they interact with several proteins in the brassinosteroid pathway such as BRI1 suppressor 1 (BSU1) and brassinosteroid insensitive 2 (BIN2) (Kim *et al.*, 2011; Sreeramulu *et al.*, 2013) as well as FLG2 (Shi *et al.*, 2013).

The model shown in Figure 5 depicts how BSK1 and cGMP may interact with BRI1 in the inactive and activated states incorporating findings obtained from the literature. In the inactive state in the absence of brassinosteroid, BRI1 forms a complex with BSK1 (Tang *et al.*, 2008; Sreeramulu *et al.*, 2013) and possibly involving BAK1 although this protein may also be interacting with BAK1-interacting receptor-like kinase 2 (BIR2) (Halter *et al.*, 2014). At this stage, the transcription factors BRASSINOZOLE RESISTANT 1 and 2 (BZR1 and BZR2) will be phosphorylated by BIN2 and this promotes association with 14-3-3 proteins and retention in the cytoplasm (Tang *et al.*, 2008; Clouse, 2011). The presence of brassinosteroid stimulates oligomerization (if not already occurring) and cross phosphorylation between BRI1 and BAK1 to form a complex (Clouse, 2011). We speculate that BRI1 in the dimerized state is more likely to generate cGMP (see discussion in (Freihat *et al.*, 2014) regarding PSKR1). Cyclic GMP induces BRI1 to phosphorylate BSK1 (Figure 4) which then dissociates from the BRI1-BAK complex. BSK1 can associate with itself and other BSKs to potentially form dimers (Sreeramulu *et al.*, 2013). Dimerization may be potentiated by BIN2 which can also phosphorylate BSK1 at sites other than serine 230 (Sreeramulu *et al.*, 2013) and the dimer is thought to act as a scaffold for BIN2 and BSU1. Possibly when BSU1 is associated with BSK1 (Kim *et al.*, 2009), it becomes a substrate for phosphorylation by CDG1 (Kim *et al.*, 2011) and activated. BSU1 is a phosphatase that catalyses the dephosphorylation of the transcription factors BZR1 and BZR2 stimulating

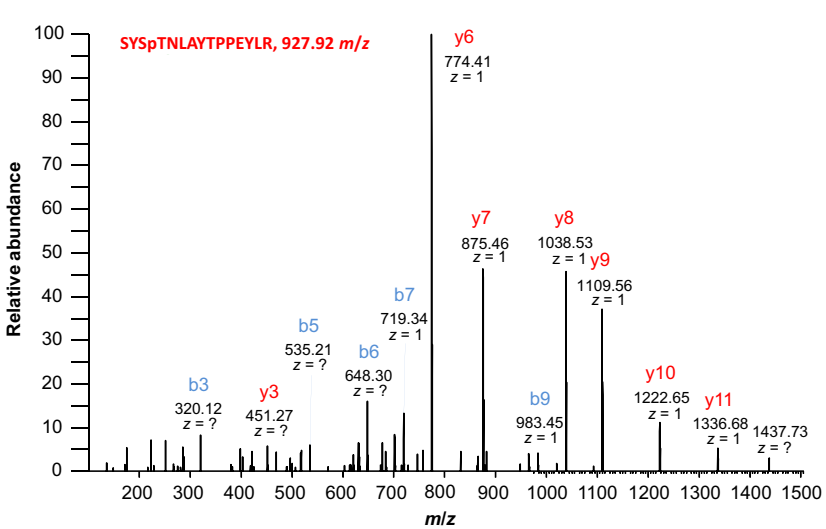

Figure 4. Phosphorylation of BSK1 is induced by cGMP.
MS2 spectrum of the BSK1 specific Ser230 phosphorylated SYSpTNLAYTPPEYLR peptide after treatment with 100 nM cGMP in cell tissue culture. BSK1 was one of the differentially expressed proteins identified. The doubly charged parent peptide has a + 49 m/z mass shift (927.92) because of the presence of an attached phospho-group. The b-ion series that arise after peptide fragmentation (MS2) show a neutral loss from b3 onwards which assign the phospho-group specifically to Ser230.

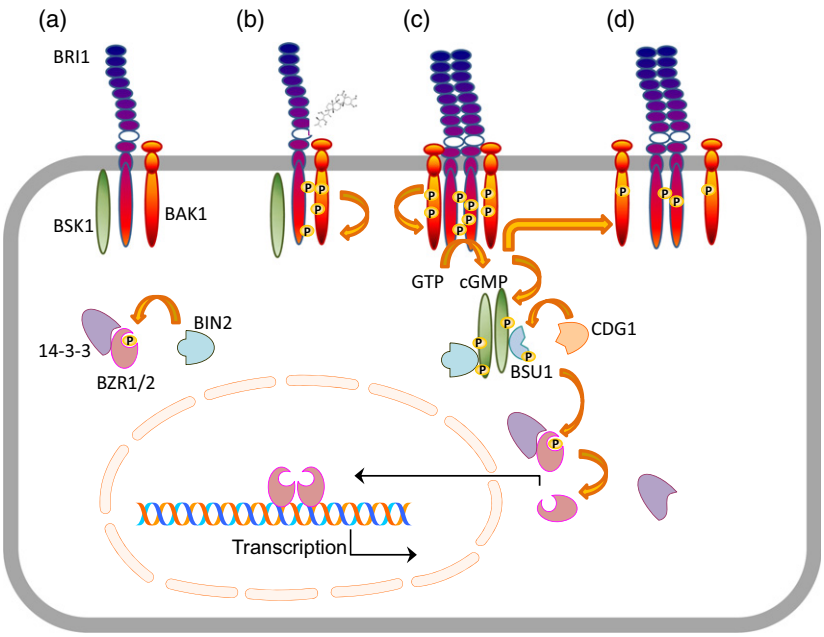

Figure 5. Model of intracellular signaling following phosphorylation and cGMP production by BRI1.
(a) BRI1, BAK1 and BSK1 assembled as inactive complex at the plasma membrane. BIN2 has phosphorylated BZR1/2 encouraging association with 14-3-3 proteins to retain BZR1/2 in cytoplasm.
(b) Brassinosteroid binds BRI1 and BAK1 to stimulate auto- and *trans*-phosphorylation.
(c) Receptor dimerization occurs resulting in cGMP production that activates BRI1 to phosphorylate BSK1 on serine 230. Phosphorylated BSK1 dissociates from the receptor complex and possibly forms a dimer to interact with BIN2 and BSU1. CDG1 can phosphorylate BSU1 and up-regulated BSU1 dephosphorylates BZR1 and BZR2 resulting in dissociation from 14-3-3 proteins. BZR1 and BZR2 can then enter the nucleus and modulate BR-responsive gene expression.
(d) Accumulation of cGMP in the receptor complex region suppresses BRI1 kinase activity and this in turn promotes complex dissociation.

dissociation of cytoplasmic complexes and entry into the nucleus and modulation of brassinosteroid dependent gene transcription (Clouse, 2011). For the sake of simplicity, we have omitted the role of additional transcription factors such as HBI1 that are positively regulated by brassinosteroids but negatively regulated by PAMP-induced immune responses (Malinovsky *et al.*, 2014) as BAK1 has a partly understood role in mediating both growth and immune responses. The cGMP formed by BRI1 also has an inhibitory effect on BRI1 kinase activity and thus acts to dampen the signal networks (Figure 5).

Using recombinant cytoplasmic protein, we have shown that BRI1 has both kinase and GC activity and while kinase activity enhances GC activity the product of GC activity, cGMP, supresses the kinase activity of BRI1. Both wild-type and the GC centre mutant full-length proteins expressed in plant tissue also exhibit kinase activity. Furthermore, we have shown that cGMP potentiates phosphorylation of the downstream target BSK1 in cells derived from Arabidopsis roots. The next challenges are to clarify the roles Y956F or G989I play in inhibiting GC activity and to determine residues specific for cGMP binding both *in vitro* and *in planta*.

EXPERIMENTAL PROCEDURES

Preparation of recombinant protein constructs

Kapa HiFi PCR (KapaBiosystems, Wilmington, MA, USA), oligonucleotides AtBRI1-fwd and AtBRI1-rev (Table S1) flanking the BRI1 coding region along with genomic DNA isolated from *Arabidopsis thaliana* (Col) (Qiagen, Hilden, Germany) were used to amplify the AtBRI1 encoding gene. This PCR product was used as template in another Kapa HiFi PCR with oligonucleotides AtBRI1cd-fwd-gw and AtBRI1-rev-gw-stop or AtBRI1fl-fwd-gw and AtBRI1-rev-gw nostop (Table S1) to amplify the respective cytoplasmic or full-length encoding domain of AtBRI1 (encoding amino acids 815–1196 or 1–1195) incorporating a start codon and Gateway recombination sites. The resulting PCR products were independently recombined into pDONR207 (Invitrogen, Carlsbad, CA, USA) to create pENTRYBRIcds and pENTRYBRIflns which were confirmed through sequencing. BRI1 mutants Y956F, G989I and G1073K were each generated using QuikChange II Site-Directed Mutagenesis kit (Stratagene, San Diego, CA, USA), while the KR1083/4AA mutant was generated using Phusion high-fidelity PCR master mix (New England BioLabs, Genesearch Australia) and digesting original vectors with Dpn1 (New England BioLabs). pENTRYBRIcds or pENTRYBRIflns was used as template and in each case mutagenesis primers were designed through http://www.genomics.agilent.com/primerDesignProgram.jsp. The individual pENTRYBRIcds and pENTRYBRIflns mutant constructs were generated using the appropriate forward and reverse oligonucleotides listed in Table S1. Each plasmid was verified through sequencing. The BRI1 cytoplasmic domain from each of pENTRYBRIcds, pENTRYBRIcdsY956F, pENTRYBRIcdsG989I, pENTRYBRIcdsG1073K and pENTRYBRIcdsKR1083/4AA was independently recombined into pDEST17 to create pDEST17BRI1cds, pDEST17BRI1cdsY956F, pDEST17BRI1cdsG989I, pDEST17BRI1cdsG1073K and pDEST17-BRI1cdsKR1083/4AA respectively and verified by sequencing. The full-length BRI1 encoding region from each of pENTRYBRIflns, pENTRYBRIflnsY956F and pENTRYBRIflnsKR1083/4AA were independently recombined into pEarleyGate103 (Earley *et al.*, 2006) to create pEarleyGate103BRI1flns, pEarleyGate103BRI1flnsY956F and pEarleyGate103BRI1flnsKR1083/4AA, respectively.

Recombinant protein preparation

For the expression of $BRI1^{815–1196}$, $BRI1^{815–1196}$Y956F, $BRI1^{815–1196}$G989I, $BRI1^{815–1196}$G1073K and $BRI1^{815–1196}$KR1083/4AA recombinant proteins the appropriate construct was transformed into One Shot BL21 (DE3)pLysS *E. coli* cells (Life Technologies, Carlsbad, CA, USA) and several independent colonies of each construct were selected, induced by adding 0.2% arabinose then grown for a further 3 h at 37°C (Muleya *et al.*, 2013). The recombinant

proteins were purified under native conditions as described in Protocols 9 and 12 of the QIAexpressionist manual (Qiagen).

Tobacco leaves and immunoprecipitation

For the expression of $BRI1^{1–1195}$, $BRI1^{1–1195}$Y956F and $BRI1^{1–1195}$KR1083/4AA proteins in tobacco the appropriate construct was transformed into *Agrobacterium tumefaciens* strain GV3101 (pMP90). *A. tumefaciens* mediated transient expression experiments (method adapted from (Thatcher *et al.*, 2016) were performed on 4–5 weeks old *Nicotiana benthamiana* plants grown at 22°C under a 16-h-light/8-h-dark photoperiod. *A. tumefaciens* strains grown in 2YT media where harvested by centrifugation and resuspended in infiltration media (10 mM MES pH 5.6; 10 mM $MgCl_2$; 150 μM acetosyringone) to a final OD_{600} of 0.5 and incubated at room temperature for 3 h. Immediately prior to infiltration, each strain was diluted in infiltration media to OD_{600} of 0.2 and infiltrated into the underside of tobacco leaves using a needleless syringe. Leaves were harvested after 2 days. Infiltrated regions were weighed, ground under liquid nitrogen and extracted in 1 ml extraction buffer (50 mM Tris–HCl pH7.5, 150 mM NaCl, 1% v/v Igepal) with 1 mM PMSF per gram of leaf tissue. Tissue was defrosted at 4°C on a rotating wheel with manual shaking every 2 min over a period of 10 min, and centrifuged at 4°C for 10 min at 2300 ***g*** before transferring the supernatant to a new tube and repeating the centrifugation step. Supernatant was immediately used in immunoprecipitation experiment or stored at −80°C until required (Hartmann *et al.*, 2015). GFP-Trap (ChromoTek, Aachen, Germany) was used to immunoprecipitate the full-length proteins as described by (Thatcher *et al.*, 2016). Isolation of full-length proteins was confirmed by immunoblot analysis probing with rabbit anti-GFP primary antibody (Thermo Fisher Scientific, San Jose, CA, USA) and goat-anti-rabbit IRDye 800CW (Li-Cor Biosciences, Millenium Science, Mulgrave, VIC, Australia) to detect GFP using the Odyssey infrared imaging system (Li-Cor Biosciences).

Assessment of GC activity

GC activity *in vitro* was assessed by measuring cGMP generated from GTP in the presence of 5 μg purified protein as previously described (Kwezi *et al.*, 2007) using the cGMP enzyme immunoassay (EIA) Biotrak System (GE Healthcare, USA) with the acetylation protocol as described in the supplier's manual or by mass spectrometry. Mass spectrometry detection and quantitation of cGMP were done on a Thermo LTQ Velos Orbitrap mass spectrometer (Thermo Fisher Scientific) that is equipped with a heated ESI ion source. The ionization source parameters were optimized in positive ESI mode using pure cGMP (Sigma, St Louis, MO, USA) dissolved in HPLC-grade water. The LC-MS/MS analysis was performed by injecting 10 μl of standard or sample onto a Sepax SFC-Cyano column (4.6 mm × 150 mm, 5 μm) (Sepax Technologies, Newark, DE, USA) and eluting in isocratic mode using a solvent mix of 10 mM ammonium acetate in 40/60 acetone nitrile/water for 5 min and at a mobile phase flow rate of 0.5 ml/min. All analyses were carried out in positive ionization mode using a metal needle with a spray voltage of 4 kV. The source vaporizing temperature and the ion transfer tube temperature were set at 310°C and 260°C, respectively. Instrument control and data analysis were performed using the Xcalibur software (Thermo Scientific, USA).

In vitro kinase assays

Kinase activity of the cytoplasmic domain of wild-type BRI1 was measured as an increase in fluorescence of the phosphorylated Sox substrate peptide (Shults and Imperiali, 2003) using the Omnia® Ser/Thr Peptide 1 kit (Life Technologies). The kinase reaction was performed in triplicate in the presence of 20 mM Tris–HCl pH 7.5, 15 mM $MgCl_2$, 1 mM ATP, 0.2 mM DTT and 1 μg of recombinant protein. Fluorescence was measured using an EnVision® 2101 multilabel plate reader (PerkinElmer, Melbourne, Australia) with excitation and emission wavelengths of 405 and 492 nm, respectively as previously described (Kwezi *et al.*, 2011). Kinase activity of wild-type and mutant recombinant proteins was compared using the peptide BR13 (Oh *et al.*, 2000) as a substrate. In brief, recombinant protein and BR13 as substrate were incubated together in buffer (50 mM HEPES pH7.5, 10 mM $MgCl_2$, 0.2 mM CaCl, 0.1 mg ml^{-1} peptide substrate, 1 μg ml^{-1} recombinant protein) with or without 5 mM ATP for 20 min and terminated by adding 75 mM H_3PO_4. The reactions containing the BR13 peptide were spotted onto nitrocellulose over a heat block set at 50°C to dry and probed with Pro-Q phosphoprotein blot stain (Thermo Fisher Scientific) and visualized with a Typhoon Trio variable imager (GE Healthcare, Buckinghamshire, UK) using a 488 nm blue laser and a 520 nm band-pass (BP) 40 emission filter. Reactions containing full-length immunoprecipitated proteins and full-length myelin basic protein (MBP) were undertaken in reaction as above and separated on 10% SDS-PAGE before staining with Pro-Q-Diamond phosphoprotein gel stain (Thermo Fisher Scientific). Phosphoprotein bands were visualized in a Typhoon Trio variable imager. Image intensities were quantified using FIJI software (http://imagej.net/Fiji/Downloads; accessed 2 June 2016) and normalised against phosphoprotein standard.

cGMP-induced phosphoproteins

Cells derived from roots of *Arabidopsis thaliana* (ecotype Columbia-0) were grown with either light (^{14}N) or heavy (^{15}N) potassium nitrate on a shaking platform (120 rpm) in Gamborg's B-5 basal salt mixture (Sigma-Aldrich) supplemented with 2,4-dichlorophenoxyacetic acid (0.5 μg ml^{-1}) and kinetin (0.05 μg ml^{-1}) in a growth chamber (Innova® 43, New Brunswick Scientific Co., NJ, USA) at 23°C under 12 h light/dark cycles as previously described (Turek *et al.*, 2014). The cell cultures were treated with 100 nM cGMP or with water (control) for 5 min. Proteins were extracted, digested and fractionated as previously described (Groen *et al.*, 2013). Phosphopeptide enrichment was undertaken as previously described (Zhang *et al.*, 2013). Enriched phosphopeptides were analysed on a Q-Exactive Orbitrap with nano-electrospray ionization (Thermo Fisher Scientific) coupled to a nanoLC Dionex Ultimate 3000 UHPLC (Thermo Fisher Scientific). Samples were trapped on a 180 μm × 20 mm, C18, 5 μm, 100 Å trapping column Acclaim PepMap 100 (Thermo Fisher Scientific) with the μl PickUp Injection mode using the loading pump at 15 μl min^{-1} flow rate for 3 min. Samples were then loaded on a RSLC, 75 μm × 500 mm, nanoViper, C18, 2 μm, 100 Å column (Acclaim, PepMap) retrofitted to an EASY-spray source with a flow rate of 300 nl min^{-1} (buffer A: HPLC-grade H_2O, 0.1% (v/v) formic acid; buffer B: 100% (v/v) ACN, 0.1% (v/v) formic acid). Peptides were eluted over a 60 min gradient (0–3 min: 2% buffer B, 3–30 min: 5 to >40% buffer B, 30–35 min: 95% buffer B, 35–60 min: 2% buffer B). Peptides were transferred to the gaseous phase with positive ion electrospray ionization at 1.8 kV. Top 20 precursors were acquired between 380 and 1600 m/z with a 1.5 precursor ion selection window, a dynamic exclusion of 20 sec, a normalised collision energy (NCE) of 25 and a resolution of 70 000 in MS1 and 17 500 in MS2. Data were recorded using Xcalibur™ software version 2.1 (Thermo Fisher Scientific) and files were converted from '.raw' to '.mzXML' using MSConvert and then '.mzXML' files to '.mgf' using iSPY (Gutteridge *et al.*, 2010). The.mgf files were then finally imported into MASCOT (Matrix Science, London, UK), with carbamidomethyl as a fixed modification, and oxidation on methionine (M) residues and

phosphorylation on serine (S), threonine (T), and tyrosine (Y) residues as variable modifications; 25 ppm of peptide tolerance, 0.8 Da of MS/MS tolerance; a maximum of two missed cleavages, a peptide charges of +2, +3, or +4; and selection of decoy database. Mascot '.dat' output files were imported into iSPY for $^{14}N/^{15}N$ quantitation and analysed through percolator for improved identification (Brosch *et al.*, 2009). The ^{14}N and ^{15}N peptide isotopic peaks from MS1 dataset were used to compare the theoretical mass difference between the heavy and light peptides, and the typical isotopic distribution patterns. After normalisation, only peptides detected in at least two biological replicates, with a fold change $|\pm 1.5|$ and a $P \leq 0.05$ were considered for further analysis.

Computational assessment of the BRI1 (Arg^{815}–Leu^{1196}) structure

The BR1 kinase domain (Arg^{815}–Leu^{1196}), BRI1 GC centre (Leu^{1021}–Arg^{1134}) and the mutants: BRI1 G1073E, BRI1 G1073K, BRI1 Y956F and BRI1 G989I were modelled against the crystal structure of the BRI1 kinase domain (PDB entry: 4OA2; Bojar *et al.*, 2014) using Modeller (ver. 9.14) (Sali and Blundell, 1993). GTP docking simulation was performed using AutoDock Vina (ver. 1.1.2) (Trott and Olson, 2010). All structures and images were analysed and prepared with UCSF Chimera (Pettersen *et al.*, 2004) and PyMOL (ver. 1.7.4) (The PyMOL Molecular Graphics System, Schrödinger, LLC, Cambridge, MA, USA).

ACCESSION NUMBERS

AtBRI1: AT4G39400; BRI1 kinase domain: PDB entry 4OA2; AtBSK1: AT4G35230.1.

ACKNOWLEDGEMENTS

Support from the Australian Research Council funding scheme (project numbers DP0878194 and DP110104164), the National Research Foundation South Africa (grant numbers 78843; IRF2009021800047) and La Trobe University School of Life Science Publication Booster Award is gratefully acknowledged. We also thank Dr Yu Hua Wang (Monash University) for preparing the G1073K mutant construct and Dr Victor Muleya (Monash University) for helpful discussions.

CONFLICT OF INTEREST

The authors declare no conflict of interest.

SUPPORTING INFORMATION

Additional Supporting Information may be found in the online version of this article.

Figure S1. The ribbon model of BRI1 GC centre (Leu^{1021}–Arg^{1134}) incorporating the KR1083/4AA mutations.

Figure S2. Kinetics of $BRI1^{815–1196}$ using the Ser/Thr peptide 1 as a substrate.

Figure S3. Phosphorylation of threonine 353 (KQEEAPSp TPQRPLSPLGEACSR) of BSK1.

Table S1. Primers used in cloning BRI1 wild-type and mutant constructs.

REFERENCES

Allerston, C.K., Von Delft, F. and Gileadi, O. (2013) Crystal structures of the catalytic domain of human soluble guanylate cyclase. *PLoS One*, **8**, e57644.

Al-Younis, I., Wong, A. and Gehring, C. (2015) The Arabidopsis thaliana K^+-uptake permease 7 (AtKUP7) contains a functional adenylate cyclase catalytic centre. *FEBS Lett.* **589**, 3848–3852.

Bojar, D., Martinez, J., Santiago, J., Rybin, V., Bayliss, R. and Hothorn, M. (2014) Crystal structures of the phosphorylated BRI1 kinase domain and implications for brassinosteroid signal initiation. *Plant J.* **78**, 31–43.

Brosch, M., Yu, L., Hubbard, T. and Choudhary, J. (2009) Accurate and sensitive peptide identification with Mascot Percolator. *J. Proteome Res.* **8**, 3176–3181.

Clouse, S.D. (2011) Brassinosteroid signal transduction: from receptor kinase activation to transcriptional networks regulating plant development. *Plant Cell*, **23**, 1219–1230.

Earley, K., Haag, J.R., Pontes, O., Opper, K., Juehne, T., Song, K.W. and Pikaard, C.S. (2006) Gateway-compatible vectors for plant functional genomics and proteomics. *Plant J.* **45**, 616–629.

Facette, M.R., Shen, Z., Bjornsdottir, F.R., Briggs, S.P. and Smith, L.G. (2013) Parallel proteomic and phosphoproteomic analyses of successive stages of maize leaf development. *Plant Cell*, **25**, 2798–2812.

Freihat, L., Muleya, V., Manallack, D.T., Wheeler, J.I. and Irving, H.R. (2014) Comparison of moonlighting guanylate cyclases – roles in signal direction? *Biochem. Soc. Trans.* **42**, 1773–1779.

Fulton, A.B. (1982) How crowded is the cytoplasm? *Cell*, **30**, 345–347.

Groen, A., Thomas, L., Lilley, K. and Marondedze, C. (2013) Identification and quantitation of signal molecule-dependent protein phosphorylation. *Methods Mol. Biol.* **1016**, 121–137.

Gutteridge, A., Pir, P., Castrillo, J.I., Charles, P.D., Lilley, K.S. and Oliver, S.G. (2010) Nutrient control of eukaryote cell growth: a systems biology study in yeast. *BMC Biol.* **8**, 68.

Halter, T., Imkampe, J., Mazzotta, S. *et al.* (2014) The leucine-rich repeat receptor kinase BIR2 is a negative regulator of BAK1 in plant immunity. *Curr. Biol.* **24**, 134–143.

Haney, C.H., Riely, B.K., Tricoli, D.M., Cook, D.R., Ehrhardt, D.W. and Long, S.R. (2011) Symbiotic rhizobia bacteria trigger a change in localization and dynamics of the *Medicago truncatula* receptor kinase LYK3. *Plant Cell*, **23**, 2774–2787.

Hartmann, J., Linke, D., Bönniger, C., Tholey, A. and Sauter, M. (2015) Conserved phosphorylation sites in the activation loop of Arabidopsis phytosulokine receptor PSKR1 differentially affect kinase and receptor activity. *Biochem. J.* **472**, 379–391.

Hothorn, M., Belkhadir, Y., Dreux, M., Dabi, T., Noel, J.P., Wilson, I.A. and Chory, J. (2011) Structural basis of steroid hormone perceptopn by the receptor kinase BRI1. *Nature*, **474**, 467–471.

Irving, H.R., Kwezi, L., Wheeler, J.I. and Gehring, C. (2012) Moonlighting kinases with guanylate cyclase activity can tune regulatory signal networks. *Plant Signal. Behav.* **7**, 201–204.

Isner, J.C., Nuhse, T. and Maathuis, F.J. (2012) The cyclic nucleotide cGMP is involved in plant hormone signalling and alters phosphorylation of Arabidopsis thaliana root proteins. *J. Exp. Bot.* **63**, 3199–3205.

Kim, T.W., Guan, S., Sun, Y., Deng, Z., Tang, W., Shang, J.-X., Sun, Y., Burlingame, A.L. and Wang, Z.-Y. (2009) Brassinosteroid signal transduction from cell-surface receptor kinases to nuclear transcription factors. *Nat. Cell Biol.* **11**, 1254–1260.

Kim, T.W., Guan, S., Burlingame, A.L. and Wang, Z.Y. (2011) The CDG1 kinase mediates brassinosteroid signal transduction from BRI1 receptor kinase to BSU1 phosphatase and GSK3-like kinase BIN2. *Mol. Cell*, **43**, 561–571.

Krügel, U., Veenhoff, L.M., Langbein, J., Wiederhold, E., Liesche, J., Friefrich, T., Grimm, B., Martinoia, E., Poolman, B. and Kühn, C. (2008) Transport and sorting of the *Solanum tuberosum* sucrose transporter SUT1 is affected by posttranslational modification. *Plant Cell*, **20**, 2497–2513.

Kwezi, L., Meier, S., Mungur, L., Ruzvidzo, O., Irving, H. and Gehring, C. (2007) The *Arabidopsis thaliana* brassinosteroid receptor (AtBRI1) contains a domain that functions as a guanylyl cyclase *in vitro*. *PLoS One*, **2**, e449.

Kwezi, L., Ruzvidzo, O., Wheeler, J.I., Govender, K., Iacuone, S., Thompson, P.E., Gehring, C. and Irving, H.R. (2011) The phytosulfokine (PSK) receptor is capable of guanylate cyclase activity and enabling cyclic GMP-dependant signaling in plants. *J. Biol. Chem.* **286**, 22580–22588.

Ladwig, F., Dahlke, R.I., Stuhrwohdldt, N., Hartmann, J., Harter, K. and Sauter, M. (2015) Phytosulfokine regulates growth in Arabidopsis through a

response module at the plasma membrane that includes CYCLIC NUCLEOTIDE-GATED CHANNEL17, H-ATPase, and BAK1. *Plant Cell*, **27**, 1718–1729.

Maathuis, F.J.M. (2006) cGMP modulates gene transcription and cation transport in Arabidopsis roots. *Plant J.* **45**, 700–711.

Malinovsky, F.G., Batoux, M., Schwessinger, B., Youn, J.H., Stransfeld, L., Win, J., Kim, S.K. and Zipfel, C. (2014) Antagonistic regulation of growth and immunity by the Arabidopsis basic helix-loop-helix transcription factor homolog of brassinosteroid enhanced expression2 interacting with increased leaf inclination1 binding bHLH1. *Plant Physiol.* **164**, 1443–1455.

Marondedze, C., Wong, A., Thomas, L., Irving, H. and Gehring, C. (2016a) Cyclic nucleotide monophosphates in plants and plant signaling. In *Handbook of Experimenal Pharmacology*, Volume 238 (Seifert, R., ed). Berlin: Springer, pp. 87–103.

Marondedze, C., Groen, A., Thomas, L., Lilley, K.S. and Gehring, C. (2016b) A quantitative phosphoproteome analysis of cGMP-dependent cellular responses in *Arabidopsis thaliana*. *Mol. Plant*, **9**, 621–623.

Muleya, V., Wheeler, J.I. and Irving, H.R. (2013) Structural and functional characterization of receptor kinases with nucleotide cyclase activity. *Methods Mol. Biol.* **1016**, 175–194.

Muleya, V., Wheeler, J.I., Ruzvidzo, O., Freihat, L., Manallack, D.T., Gehring, C. and Irving, H.R. (2014) Calcium is the switch in the moonlighting dual function of the ligand-activated receptor kinase phytosulfokine receptor 1. *Cell Commun. Signal.* **12**, 60.

Muleya, V., Marondedze, C., Wheeler, J.I. *et al.* (2016) Phosphorylation of the dimeric cytoplasmic domain of the phytosulfokine receptor, PSKR1. *Biochem. J.* **473**, 3081–3098.

Oh, M.-H., Ray, W.K., Hiber, S.C., Asara, J.M., Gage, D.A. and Clouse, S.D. (2000) Recombinant brassinosteroid insensitive 1 receptor-like kinase autophosphorylates on serine and threonine residues and phosphorylates a conserved peptide motif *in vitro*. *Plant Physiol.* **124**, 751–765.

Oh, M.-H., Wang, X., Kota, U., Goshe, M.B., Clouse, S.D. and Huber, S.C. (2009) Tyrosine phosphorylation of the BRI1 receptor kinase emerges as a component of brassinosteroid signaling in *Arabidopsis*. *Proc. Natl Acad. Sci. USA*, **106**, 658–663.

Pettersen, E.F., Goddard, T.D., Huang, C.C., Couch, G.S., Greenblatt, D.M., Meng, E.C. and Ferrin, T.E. (2004) UCSF Chimera–a visualization system for exploratory research and analysis. *J. Comput. Chem.* **25**, 1605–1612.

Qi, Z., Verma, R., Gehring, C., Yamaguchi, Y., Zhao, Y., Ryan, C.A. and Berkowitz, G.A. (2010) Ca^{2+} signaling by plant *Arabidopsis thaliana* Pep peptides depends on AtPepR1, a receptor with guanylyl cyclase activity, and cGMP-activated Ca^{2+} channels. *Proc. Natl Acad. Sci. USA*, **107**, 21193–21198.

Rauch, A., Leipelt, M., Russwurm, M. and Steegborn, C. (2008) Crystal structure of guanylyl cyclase Cya2. *Proc. Natl Acad. Sci. USA*, **105**, 15720–15725.

Reiland, S., Messerli, G., Baerenfaller, K., Gerrits, B., Endler, A., Grossmann, J., Gruissem, W. and Baginsky, S. (2009) Large-scale Arabidopsis phosproteome profiling reveals novel chloroplast kinase substrates and phosphorylation networks. *Plant Physiol.* **150**, 889–903.

Sali, A. and Blundell, T. (1993) Comparative protein modeling by satisfaction of spatial restraints. *J. Mol. Biol.* **234**, 779–781.

Shi, H., Shen, Q., Qi, Y., Yan, H., Nie, H., Chen, Y., Zhao, T., Katagiri, F. and Tang, D. (2013) BR-SIGNALING KINASE1 physically associates with FLAGELLIN SENSING2 and regulates plant innate immunity in *Arabidopsis*. *Plant Cell*, **25**, 1143–1157.

Shiu, S.-H., Karlowski, W.M., Pan, R., Tzeng, Y.-H., Mayer, K.F.X. and Li, X.-H. (2004) Comparitive analysis of the receptor-like kinase family in Arabidopsis and rice. *Plant Cell*, **16**, 1220–1234.

Shults, M.D. and Imperiali, B. (2003) Versatile fluorescent probes of protein kinase activity. *J. Am. Chem. Soc.* **125**, 14248–14249.

Spitzer, J. and Poolman, B. (2013) How crowded is the prokaryotic cytoplasm? *FEBS Lett.* **587**, 2094–2098.

Sreeramulu, S., Mostizky, Y., Sunitha, S. *et al.* (2013) BSKs are partially redundant positive regulators of brassinosteriod signaling in Arabidopsis. *Plant J.* **74**, 905–919.

Sun, Y., Han, Z., Tang, J., Hu, Z., Chai, C., Zhou, B. and Chai, J. (2013) Structure reveals that BAK1 as a co-receptor recognises the BRI1-bound brassinolide. *Cell Res.* **23**, 1326–1329.

Tang, W., Kim, T.W., Oses-Prieto, J.A., Sun, Y., Deng, Z., Zhu, S., Wang, R., Burlingame, A.L. and Wang, Z.Y. (2008) BSKs mediate signal transduction from the receptor kinase BRI1 in Arabidopsis. *Science*, **321**, 557–560.

Thatcher, L.F., Cevik, V., Grant, M., Zhai, B., Jones, J.D.G., Manners, J.M. and Kazan, K. (2016) Characterization of a *JAZ7* activation-tagged Arabidopsis mutant with increased susceptibility to the fungal pathogen *Fusarium oxyspoum*. *J. Exp. Bot.* **67**, 2367–2386.

Trott, O. and Olson, A.J. (2010) AutoDock Vina: improving the speed and accuracy of docking with a new scoring function, efficient optimization, and multithreading. *J. Comput. Chem.* **31**, 455–461.

Turek, I. and Gehring, C. (2016) The plant natriuretic receptor is a guanylyl cyclase and enables cGMP-dependent signaling. *Plant Mol. Biol.* **91**, 275–286.

Turek, I., Marondedze, C., Wheeler, J., Gehring, C. and Irving, H. (2014) Plant natriuretic peptides induce proteins diagnostic for an adaptive response to stress. *Front. Plant Sci.* **5**, 661.

Winger, J.A., Derbyshire, E.R., Lamers, M.H., Marletta, M.A. and Kuriyan, J. (2008) The crystal structure of the catalytic domain of a eukaryotic guanylate cyclase. *BMC Struct. Biol.* **8**, 42.

Wong, A. and Gehring, C. (2013) The *Arabidopsis thaliana* proteome harbors undiscovered multi-domain molecules with functional guanylyl cyclase catalytic centers. *Cell Commun. Signal.* **11**, 48.

Wong, A., Gehring, C. and Irving, H.R. (2015) Conserved functional motifs and homology modeling to predict hidden moonlighting functional sites. *Front. Bioeng. Biotechnol.* **3**, 82.

Xu, W., Huang, J., Li, B., Li, J. and Wang, Y. (2008) Is kinase activity essential for biological functions of BRI1? *Cell Res.* **18**, 472–478.

Zhang, H., Zhou, H., Berke, L., Heck, A.J., Mohammed, S., Scheres, B. and Menke, F.L. (2013) Quantitative phosphoproteomics after auxin-stimulated lateral root induction identifies an SNX1 protein phosphorylation site required for growth. *Mol. Cell. Proteomics*, **12**, 1158–1169.

